The Plant Journal (2002) **32**, 1023–1032

The stability of cortical microtubules depends on their orientation

Bodo Wiesler, Qi-Yan Wang and Peter Nick*
Institut für Biologie II/Botanik, Schänzlestrasse 1, Universität Freiburg, D-79104 Freiburg, Germany

Received 22 July 2002; revised 10 September 2002; accepted 18 September 2002.
*For correspondence (fax +49 761 203 2612; e-mail peter.nick@biologie.uni-freiburg.de).

Summary

Auxin controls the orientation of cortical microtubules in maize coleoptile segments. We used tyrosinylated α-tubulin as a marker to assess auxin-dependent changes in microtubule turnover. Auxin-induced tyrosinylated α-tubulin, correlated with an elevated sensitivity of growth to antimicrotubular compounds such as ethyl-*N*-phenylcarbamate (EPC). We determined the affinity of α-tubulin to EPC and found that it was dramatically increased when the tubulin was de-tyrosinylated. By proteolytic cleavage of the carboxy terminal tyrosine, such an increased affinity could be induced *in vitro*. Thus, the auxin-induced sensitivity of growth to EPC is not caused by an increased affinity for this inhibitor, but caused by a reduced microtubule turnover. Double visualization assays revealed that the transverse microtubules induced by auxin consist predominantly of tyrosinylated α-tubulin, whereas the longitudinal microtubules induced by auxin depletion contain de-tyrosinylated α-tubulin. The results are discussed in terms of direction-dependent differences in the lifetime of microtubules.

Abbreviations: IAA, indolyl-3-acetic acid; MAP, microtubule-associated protein.

Keywords: auxin, de-tyrosination, maize, microtubules, post-translational modification, tubulin.

Introduction

Cortical microtubules define the direction of cellulose deposition and thus determine the preferential axis of cell growth in plant tissues. The transverse microtubules characteristic for elongating cells can re-orient in response to a panel of endogenous and exogenous signals such as light, gravity, plant hormones, abiotic and biotic stresses (for review, see Nick, 1998), accompanied by corresponding changes in the proportionality of cell expansion.

The mechanism of microtubule re-orientation has long been discussed in terms of an actual movement of assembled microtubules. A very elegant model (Lloyd and Seagull, 1985) proposed that the cortical microtubules constitute a mechanical entity that corresponds to a dynamic spring. By releasing or increasing the tension in this spring (caused by mutual sliding of the constituting microtubules), the pitch of this helix would change between transverse and longitudinal. However, when microtubules were visualized in living plant cells by microinjecting fluorescent tubulin, the lifetime of individual microtubules was found to be extremely short (Yuan *et al.*, 1994), which was difficult to reconcile with the concept of a mechanically coupled spring. Moreover, the transitional state was observed to consist of a criss-cross situation where transverse and longitudinal microtubules co-exist. In contrast, the dynamic-spring model would have predicted parallel arrays of oblique microtubules. In maize coleoptiles, these mixed arrays could be induced by gravity and followed *in vivo* (Himmelspach *et al.*, 1999). These studies led to a two-phase model of microtubule re-orientation (for review, see Lloyd, 1994) where the actual re-orientation involves direction-dependent changes of microtubule lifetime (i.e. longitudinal microtubules acquire increased stability, whereas transverse microtubules become labile), and the re-oriented, disordered microtubules subsequently co-align into a new parallel array. From the mechanistic point of view, the first phase would require changes in the activity of structural microtubule-associated proteins (MAPs) that control the lifetime of a given microtubule, whereas the second phase would be driven by microtubule motors.

A central prerequisite of this model would be differences in the lifetime of microtubules that are dependent on some

kind of vector, i.e. orientation with respect to the cell axis. The direction of this unknown vector would then change in response to the signal that triggers microtubular re-orientation.

The stability of microtubules is generally believed to depend on the activity of structural MAPs that decrease the frequency of microtubule catastrophe (Bin-Bing and Kirschner, 1999; Caudron *et al.*, 2000). Stable microtubules have been observed in both animals and plants to consist of tubulin that is post-translationally modified (for review, see MacRae, 1997). All α-tubulins, with the exception of one species (the slime mould *Physarum polycephalum*; Watts *et al.*, 1987), carry a carboxy terminal tyrosine, which can be post-translationally cleaved off by a tubulin tyrosine carboxypeptidase. The carboxy terminal tyrosine can be restored by a tubulin tyrosine ligase. The biological role of this de-tyrosination process is not understood, but in mammalian cells, microtubules consisting of de-tyrosinylated tubulin are less dynamic (Kreis, 1987). The initial model assumed that the de-tyrosinylated tubulin was the cause for the increased stability. However, it turned out later that the tubulin tyrosine carboxypeptidase, responsible for this modification, preferentially binds to tubulin that is assembled in microtubules, whereas it shows less affinity for dimeric tubulin. Conversely, the tubulin tyrosine ligase acts predominantly on dimeric tubulin (Kumar and Flavin, 1981). This would favour an alternative scenario where tubulin tyrosination would primarily depend on microtubule dynamics (Khawaja *et al.*, 1988). In fact, the dynamics of microtubules assembled *in vitro* from tyrosinylated or de-tyrosinylated tubulin is indistinguishable (Skoufias and Wilson, 1998).

De-tyrosination has been described for plant tubulin as well and can be triggered by signals that control growth (Duckett and Lloyd, 1994). Although it is not known whether de-tyrosination is cause or consequence of microtubule stability, it can be used as marker for microtubules with increased lifetime. There exist a couple of well-characterized monoclonal antibodies that detect tyrosinylated tubulin (Kilmartin *et al.*, 1982; Kreis, 1987). We therefore ventured to ask whether signal-triggered microtubule re-orientation involves direction-dependent differences of microtubule lifetime. In the present work, we demonstrate that de-tyrosination can be controlled via auxin, a well-known regulator of microtubule orientation in plants. We further describe a simple one-step protocol by which the tyrosinylated and de-tyrosinylated forms of plant α-tubulin can be separated and show that this discrimination depends exclusively on the carboxy terminal tyrosine. We observe that the longitudinal microtubules produced in response to auxin depletion predominantly contain the de-tyrosinylated form of α-tubulin, indicating direction-dependent differences of microtubule stability.

Results

De-tyrosination of tubulin can be triggered by auxin depletion

When segments from maize coleoptiles are depleted from endogenous auxin, they stop growing. Elongation can be recovered by addition of exogenous auxin (indolyl-3-acetic acid, IAA) to the medium with maximal growth for 5 μM as shown in Figure 1(a). Incubation with increasing concentrations of the antimicrotubular herbicide ethyl-*N*-phenylcarbamate (EPC; Mizuno and Suzaki, 1990) progressively inhibits elongation (Figure 1b). However, 10-fold higher concentrations of EPC are required to inhibit growth when only 0.1 μM IAA is present as compared to the optimal concentration (5 μM IAA). This is not caused by differences

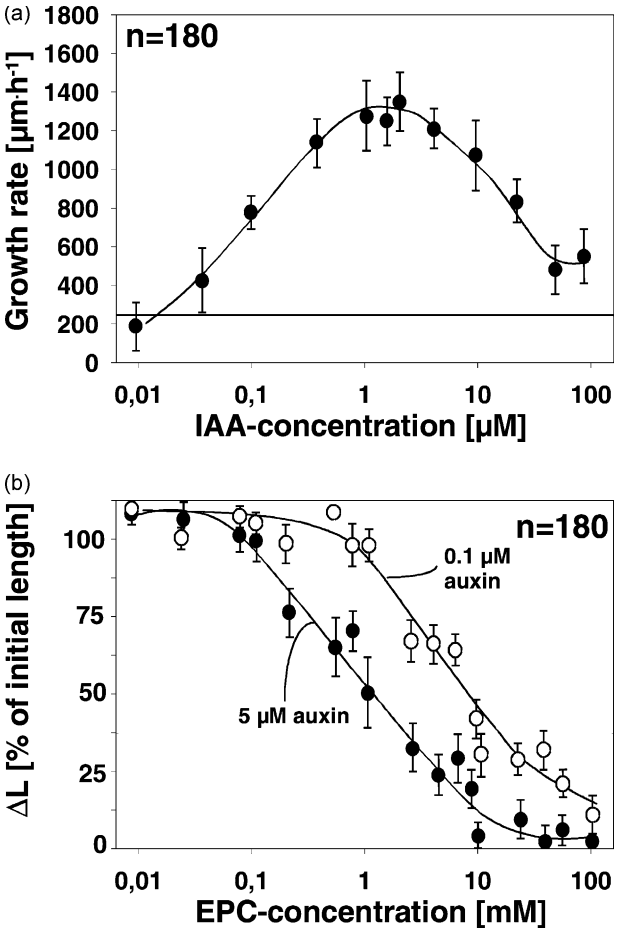

Figure 1. The sensitivity of growth to the microtubule assembly blocker, ethyl-*N*-phenylcarbamate (EPC), depends on auxin.
(a) Dose–response for auxin-induced growth in maize coleoptile segments.
(b) Dose–response for inhibition of growth by the microtubule assembly blocker, ethyl-*N*-phenylcarbamate (EPC), in the presence of 5 μM (closed circles) or 0.1 μM (open circles) of IAA. To obtain the same growth increment in the controls, the incubation at 0.1 μM took place at 30°C (in contrast to 25°C for the incubation at 5 μM).

Table 1 Inhibition of cell elongation by antimicrotubular drugs in the presence of suboptimal (0.1 μM) versus optimal (5 μM) concentrations of IAA

	Relative increment in original segment length (%)	
	0.1 μM IAA	5 μM IAA
EPC (mM)		
0.1	105 ± 4	99 ± 3
1	98 ± 5	52 ± 1
10	32 ± 2	5 ± 2
IPC (mM)		
0.01	93 ± 3	101 ± 4
0.1	105 ± 4	59 ± 3
1	22 ± 2	7 ± 2
Colchicin (mM)		
0.5	105 ± 5	89 ± 3
5	99 ± 4	61 ± 2
50	62 ± 3	12 ± 3
Oryzalin (mM)		
0.05	100 ± 3	106 ± 4
0.5	91 ± 3	39 ± 2
5	49 ± 4	15 ± 4
Trifluralin (mM)		
0.05	103 ± 7	91 ± 5
0.5	92 ± 7	44 ± 8
5	22 ± 7	2 ± 1

To obtain the same absolute growth increments in the controls, the incubation at 0.1 μM took place at 30°C (in contrast to 25°C for the incubation at 5 μM). Twenty-five individual segments were measured for each data point.

of initial growth rate, since these were equalized by incubating the segments at higher temperature (30°C) for the suboptimal concentration. The same effect was observed when other antimicrotubular drugs such as colchicin, oryzalin, trifluralin or isopropyl-*N*-phenylcarbamate were used. Table 1 shows that higher concentrations were required to inhibit growth when only 0.1 μM IAA were present.

To understand these auxin-dependent differences in the sensitivity of growth to antimicrotubular drugs, the expression of α-tubulin was checked in presence or absence of exogenous auxin using three commercially available monoclonal antibodies raised against mammalian neurotubulin. As shown in Figure 2(a), the DM1A antibody (Breitling and Little, 1986) recognizes an epitope present in all isotypes of maize α-tubulin known so far. The ATT antibody (Kreis, 1987) was raised against the C-terminus of tyrosinylated pig brain α-tubulin, and the binding of the YL1/2 antibody predominantly depends on the presence of the carboxy terminal glutamate/aspartate-tyrosine dimer of α-tubulin that is preserved in all maize isotypes (Wehland and Willingham, 1983). When total extracts from auxin-depleted and auxin-treated segments were compared, the signal recognized by DM1A was found to be unchanged (Figure 2b). In contrast, the level of the epitope recognized by ATT antibody was low in the absence of auxin, but high after the addition of auxin. This indicates that in the absence of auxin, most tubulin is de-tyrosinylated. To test the possibility that in the absence of auxin other isotypes are abundant that might not be recognized by the ATT antibody, the

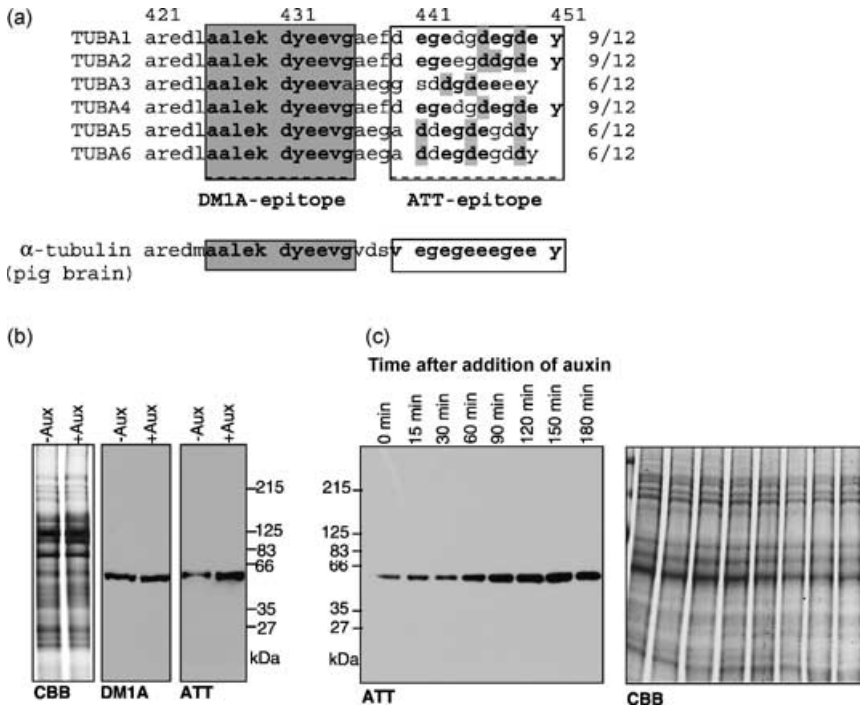

Figure 2. Detection of tyrosinylated and de-tyrosinylated maize α-tubulin in extracts from coleoptile segments that had been depleted from endogenous auxin or complemented with exogenous auxin.
(a) C-terminal sequences of all known maize α-tubulin isotypes in comparison to α-tubulin from pig brain with the locations of the epitope recognized by DM1A (gray box) and ATT (open box). The number of conserved amino acids (identical and conserved exchanges) between maize and porcine tubulin within the ATT epitope is indicated at the end of each line.
(b) Reduction of the ATT epitope relative to the DM1A in response to auxin depletion for 3 h.
(c) Induction of the ATT epitope by addition of exogenous auxin in pre-depleted segments. Ten micrograms of total protein loaded per lane. CBB, Coomassie Brilliant Blue stain of replica of the blotted gels; ATT, DM1A, Western blots probed with the ATT and DM1A antibodies.

YL1/2 antibody was used as a control with the same result (data not shown).

The induction of tyrosinylated α-tubulin by auxin was followed over time (Figure 2c). Induction can be detected from about 1 h after addition of auxin, reaching a maximum at 2–2.5 h.

Tyrosinylated and de-tyrosinylated tubulin differ in their affinity for EPC

The higher resistance of growth to EPC after depletion from endogenous auxin might be caused by a reduced affinity of the de-tyrosinylated α-tubulin dominating under this condition. To test this idea, the affinity was measured by EPC affinity chromatography (Freudenreich and Nick, 1998). Carboxylated EPC was coupled to aminoethyl-sepharose and incubated with soluble plant extract. The bound proteins were fractionated by elution with increasing ionic strength. The principle of this method is shown in Figure 3(a). A protein duplet of about 50 kDa apparent molecular weight is purified by this approach (Figure 3b, arrow). When such elution profiles are probed with DM1A and ATT, one can discriminate between two populations of α-tubulin with different affinity to EPC (Figure 3d,e): The protein recognized by ATT is only weakly bound to EPC, whereas the protein recognized by DM1A binds very tightly. The protein recognized by DM1A is slightly smaller in apparent molecular weight (Figure 3c). To compare how these populations of α-tubulin respond to changes in auxin content, extracts were fractionated from auxin-depleted versus auxin-treated segments and the profiles probed simultaneously with the two antibodies (Figure 3f,g). The tightly bound tubulin population was found to be elevated upon depletion from endogenous auxin (Figure 3e), whereas after addition of 5 μM auxin, the weakly bound fraction was more abundant (Figure 3f).

The carboxy terminal tyrosine defines the affinity of α-tubulin to EPC

The fraction eluted by 0.1 M KCl from an EPC sepharose column originating from freshly excised coleoptiles (Figure 3c) was concentrated, de-salted and then used to assemble microtubules by addition of magnesium, GTP and incubation at 30°C. Figure 4(a) shows that the resulting sediment predominantly contained a protein of about 50 kDa apparent molecular weight. By treatment with carboxypeptidase A, this sedimented protein was progressively

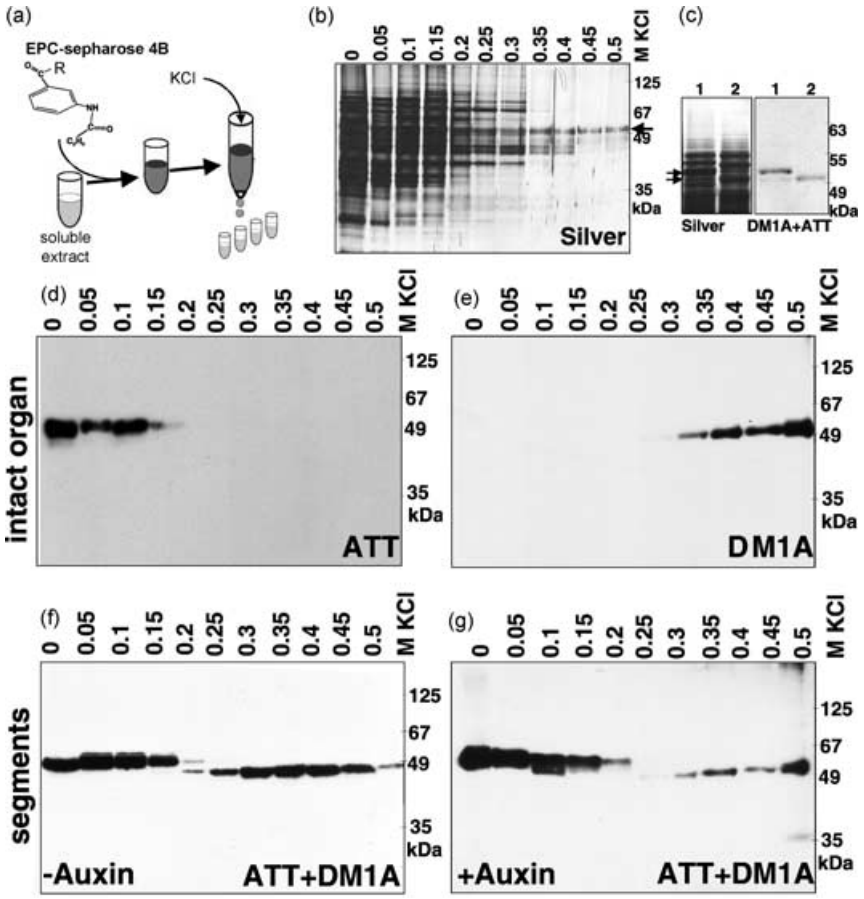

Figure 3. Separation of tyrosinylated and de-tyrosinylated maize α-tubulin by EPC sepharose affinity chromatography.
(a) Principle of the method.
(b,d,e) EPC fractionation profile obtained from freshly excised coleoptiles. (b) silver stained SDS-PAGE gel, (d) Western blot probed for ATT and (e) Western blot probed for DM1A.
(c) Comparison of α-tubulin present in the fraction eluted by 0.1 M KCl (lane 1) as compared to the α-tubulin present in the fraction eluted by 0.4 M KCl (lane 2) probed simultaneously with DM1A and ATT.
(f,g) EPC fractionation profiles probed simultaneously for ATT and DM1A from segments that had been depleted from endogenous auxin for 3 h (e) or complemented with exogenous auxin for the same time interval (f). Ten micrograms of total protein loaded per lane, except for (c) where 2 μg has been loaded. CBB, Coomassie Brilliant Blue stain of replica of the blotted gels.

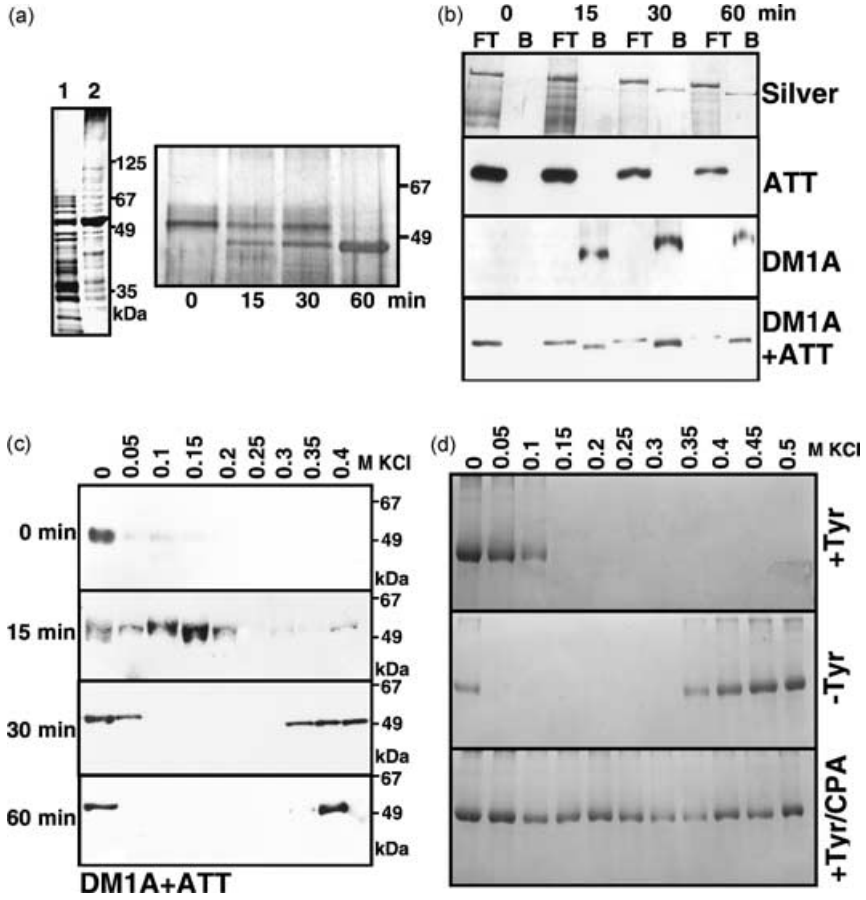

Figure 4. A high affinity of tyrosinylated α-tubulin to EPC can be induced when the tubulin is de-tyrosinated *in vitro* using carboxypeptidase A.

(a) Purification of tyrosinylated α-tubulin and de-tyrosination *in vitro*. The 0.05–0.1 M KCl fraction from an EPC fractionation profile with extracts from freshly excised segments (shown in lane 1 of the silver-stained gel) was used to assemble microtubules by GTP, magnesium and incubation at 30°C (lane 2). These were then treated for variable time intervals with carboxypeptidase A (the gel at the right side shows the re-solubilized products). The gels are stained with silver.

(b) Appearance of de-tyrosinylated α-tubulin during treatment with carboxypeptidase A. The re-solubilized proteins shown in (a) were assayed for binding to EPC. FT, flowthrough; B, bound fraction.

(c) Induction of EPC affinity in α-tubulin with increasing time of carboxypeptidase A treatment.

(d) Silver-stained EPC fractionation profile for ovalbumin conjugated to the carboxy terminal 13 amino acid residues of maize TUBA2 for a peptide either containing (+Tyr) or lacking (−Tyr) the C-terminal tyrosine. +Tyr/CPA, profile for the tyrosine containing peptide that has been pre-treated with carboxypeptidase A. Two micrograms of total protein loaded per lane throughout.

modified to yield a protein of slightly reduced molecular weight. This modification was complete within 1 h of treatment (Figure 4a). Both proteins could be completely solubilized and were then assayed for their binding to EPC sepharose (Figure 4b). The original protein of higher molecular weight was observed to remain in the unbound fraction, whereas the modified, smaller protein was tightly bound to EPC sepharose. A Western blot analysis of these fractions revealed that the original protein was recognized by ATT, but not by DM1A antibody, whereas the modified, smaller protein was recognized by DM1A, but not by ATT. When the affinities of the two proteins were measured by running complete EPC affinity profiles (Figure 4c), a progressive shift of α-tubulin from the weakly bound form (recognized by ATT) to the tightly bound form (recognized by DM1A) was observed. To test whether the affinity of α-tubulin to EPC depends on protein domains outside the carboxy terminus, the carboxy terminal peptide of the maize TUBA2 protein, the isotype most abundant in maize seedlings (Joyce *et al.*, 1992), was synthetized and conjugated to ovalbumin as carrier either with or without the carboxy terminal tyrosine (Figure 4d). This peptide could confer EPC affinity to the ovalbumin carrier depending on the carboxy terminal tyrosine: when this tyrosine was present, the binding was weak; when it was absent, the binding was strong. When the carboxy terminal tyrosine was cleaved off by carboxypeptidase A, the ovalbumin carrier was distributed into a tightly and a weakly bound subpopulation.

Tyrosinylated α-tubulin is predominantly associated with transverse microtubules

To test whether the tyrosination of α-tubulin depends on the direction of individual microtubules, mixed arrays of transverse and longitudinal microtubules were double-labelled with DM1A and ATT. To obtain such arrays, coleoptile segments were fixed 30 min after excision when many cells passed through the transition between the transverse and the longitudinal orientation (Nick *et al.*, 1990).

Since both monoclonal antibodies originate from mice, the ATT epitope was visualized first using conventional indirect immunofluorescence. Then, the DM1A epitope was visualized by direct immunofluorescence using FITC-conjugated DM1A. This protocol excludes that the ATT signal is influenced by cross-reactions with the DM1A antibody, because it has been administered first. The protocol used for the double visualization (Nick *et al.*, 1995) includes

extensive blocking, efficiently suppressing recognition of antibodies by the subsequently administered DM1A (which is a monoclonal antibody against tubulin). Figure 5(a) shows epidermal cells that had been simultaneously probed with the two antibodies during different stages of the response to auxin depletion (0, 30 and 60 min after excision) and controls (Figure 5a, right-hand column) where auxin-depleted cells with longitudinal microtubules were probed with each antibody individually. These controls show that the patterns observed for double visualization are not different from those observed for individual visualization, excluding cross-contaminations of the signals or cross-talking between the channels.

The transverse microtubules prevailing at the time of excision (0 min) were recognized by the two antibodies to about the same extent. This situation changed 30 min after depletion from auxin when cells with longitudinal and transverse microtubule arrays co-existed. Here, the longitudinal microtubules were only poorly stained by ATT, whereas transverse microtubules were clearly visualized. The transitional period, when transverse and longitudinal microtubules co-exist in the same cell, is very short (Himmelspach

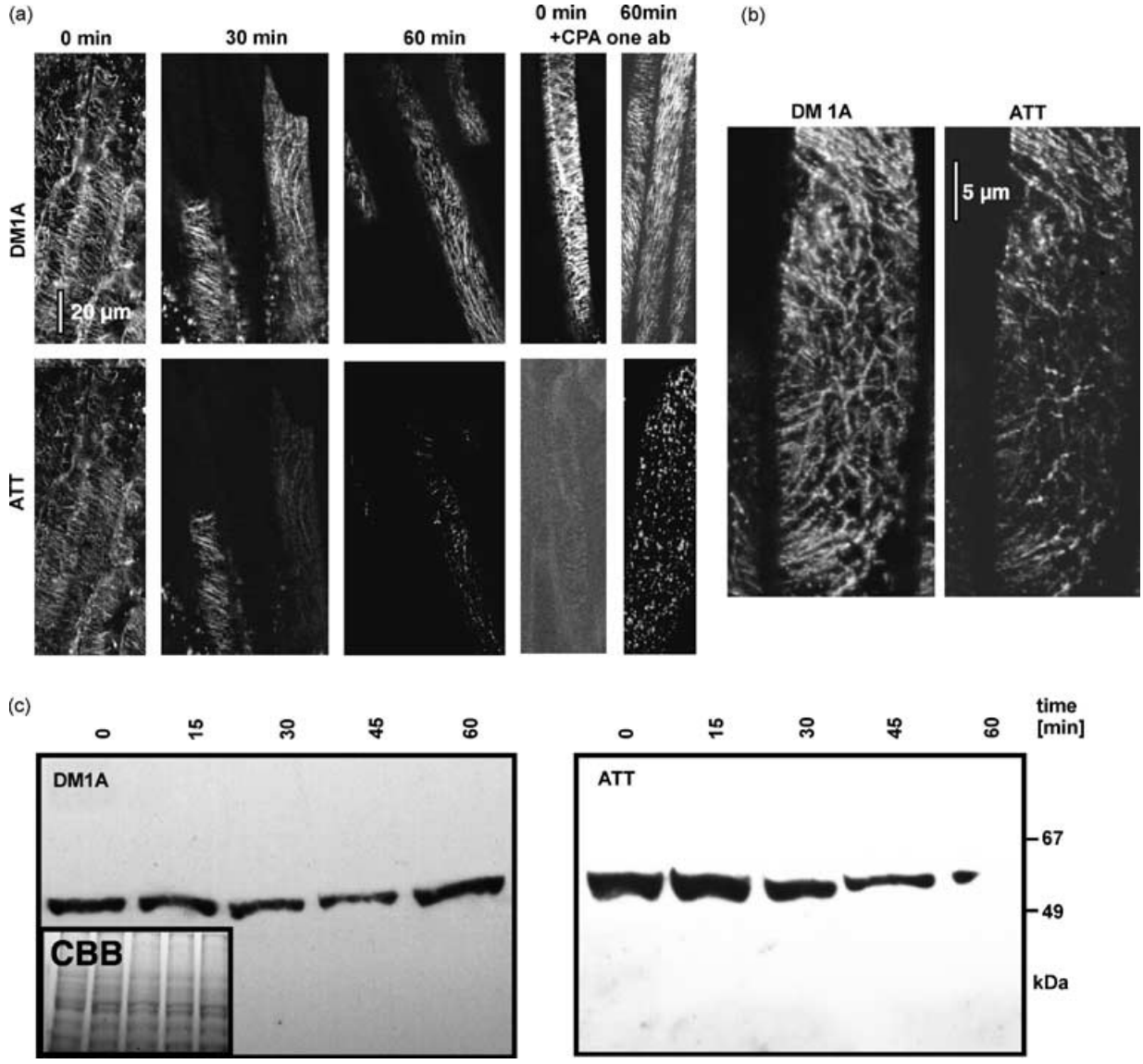

Figure 5. Double visualization of the ATT and DM1A epitope in epidermal cells of maize coleoptiles depleted from endogenous auxin.
(a) Time course for the disappearance of the ATT signal. 0 min + CPA, section from a freshly excised segment that had been treated with carboxypeptidase A prior to incubation with the primary antibody; 60 min one ab, section from a segment that had been depleted from endogenous auxin for 60 min and stained individually either with DM1A or with ATT.
(b) Detail of a cell with co-existing longitudinal and transverse microtubules fixed at 30 min after excision.
(c) Extracts from segments treated in parallel to those shown in (a) probed for DM1A and ATT. CBB, replicon of the blotted gels stained with Coomassie Brilliant Blue. Ten micrograms of total protein loaded per lane.

et al., 1999) such that it is usually hard to detect cells with mixed microtubule arrays. However, when the re-orientation process is triggered simultaneously in all cells by rapid depletion from endogenous auxin, a large part of the population is passing simultaneously through this transition at a certain time point (30 min after decapitation for the conditions used here). When the segments were fixed during this relatively short-lived transition, the ATT label is preferentially found along with transverse or oblique microtubules, whereas longitudinal microtubules were only scarcely decorated (Figure 5b). Sixty minutes after decapitation, microtubules had become longitudinal in the majority of cells. Now, the microtubules were only scarcely decorated by ATT in a punctate manner. When a sample from freshly excised coleoptiles was pre-treated with carboxypeptidase A prior to immunodetection, the ATT signal was completely removed (Figure 5a, lane 0 min - + CPA). A Western analysis (Figure 5c) in parallel subsets of these segments reveals that the disappearance of the ATT signal in the double-visualization analysis is accompanied by a general decrease of tyrosinylated α-tubulin.

Discussion

The binding site of EPC is located at the C-terminus of α-tubulin

Tyrosinylated and de-tyrosinylated α-tubulin could be separated by affinity chromatography on an EPC sepharose column (Figure 3). This suggests that the affinity to this drug depends on the presence or absence of the carboxy terminal tyrosine. When tyrosinylated α-tubulin was de-tyrosinylated *in vitro* by a commercially available carboxypeptidase, the de-tyrosinylated product acquired high EPC affinity (Figure 4). The carboxy terminal 13 amino acids of maize TUBA2 (the most common isoform in coleoptiles; Joyce *et al.*, 1992) conferred high EPC affinity to an ovalbumin carrier when the carboxy terminal tyrosine was lacking, but not when it was present (Figure 4d). However, high EPC affinity could be generated when the carboxy terminal tyrosine was cleaved off by carboxypeptidase A.

Thus, the binding site of EPC is located in the last 13 amino acids of α-tubulin. This binding site is masked in presence of the carboxy terminal tyrosine and uncovered by de-tyrosination (*in vitro* by treatment with carboxypeptidase A; *in vivo* probably by a tubulin tyrosine carboxypeptidase).

Auxin inhibits de-tyrosination of α-tubulin and maintains microtubule turnover

The abundance of tyrosinylated α-tubulin is controlled by auxin (Figure 2b,c). In intact coleoptiles (where auxin is present in concentrations that are not saturating for growth), a part of the α-tubulin is present in the tyrosinylated form that shows a low affinity for EPC and a part in the de-tyrosinylated form that binds EPC with high affinity (Figure 3d,e). By depleting the coleoptiles from endogenous auxin, the tyrosinylated α-tubulin is changed to the de-tyrosinylated form. This change can be suppressed by addition of auxin (Figure 3f,g). The most straightforward interpretation of these data is that auxin suppresses the de-tyrosination of α-tubulin by a putative tubulin tyrosine carboxypeptidase (Kumar and Flavin, 1981).

If this interpretation holds true, one would predict that microtubule dynamics is reduced in response to auxin depletion. To monitor global changes in microtubule dynamics, the sensitivity of a microtubule-driven function (cell elongation) to blockers of assembly, such as EPC, was used as indicator. The dose–response curve for EPC was shifted by about one order of magnitude to higher concentrations when the concentration of auxin was suboptimal (Figure 1); similar results were obtained for colchicin, oryzalin, trifluralin or isopropyl-*N*-phenylcarbamate (Table 1). Since the affinity of tyrosinylated α-tubulin to EPC is lower than that of de-tyrosinylated tubulin (Figure 3), one would expect a reduced sensitivity of growth in the presence of auxin (when tyrosinylated α-tubulin is more abundant). Moreover, other compounds that act on different binding sites on α- and β-tubulin were found to show the same phenomenon (Table 1) such that the drug sensitivity of growth in presence of auxin cannot be explained in terms of changed affinity. All these drugs act through the same mode of action (Mizuno and Suzaki, 1991): they block the addition of tubulin dimers to the growing end of a microtubule. Thus, a dynamic microtubule with high turnover will be more sensitive to such drugs as compared to a stable microtubule with a low rate of dimer exchange.

At low concentrations of auxin, growth is less sensitive to microtubule assembly blockers. This can be understood in terms of a reduced turnover of microtubules. The reduced turnover would increase the exposure of tubulin to tubulin tyrosine carboxypeptidase stimulating the formation of de-tyrosinylated α-tubulin. This explains the higher abundance of de-tyrosinylated tubulin in response to auxin depletion.

Does the lifetime of a microtubule depend on its orientation?

The model presented above links abundance of tyrosinylated α-tubulin to auxin-dependent microtubule dynamics. Microtubules change orientation from transverse to longitudinal in parallel to a decrease of tubulin tyrosination (Figure 5). The transition between these two orientations is not smooth in the sense of oblique arrays all over the tissue, but patchy with transverse and longitudinal arrays

co-existing in neighbouring cells (Figure 5a). Even within a given cell, longitudinal and transverse microtubules co-exist during the initial phases of re-orientation, consistent with *in vivo* observations of the re-orientation process (Himmelspach *et al*., 1999; Yuan *et al*., 1994). Double-visualization by DM1A and ATT during this re-orientation response shows that tyrosinylated tubulin is abundant in the transverse microtubules that prevail at the beginning, whereas it is hardly detectable in the longitudinal microtubules at the completion of the re-orientation (Figure 5a,b). In those cells where transverse and longitudinal microtubules co-exist, the transverse microtubules contain more tyrosinylated tubulin than the longitudinal microtubules. This, by the way, discounts the possibility that the difference in tyrosination is caused through the suppression of a (putative) tubulin tyrosine carboxypeptidase by auxin. The difference is rather innate to individual microtubules.

Again, the most straightforward explanation would be that longitudinal microtubules live longer as compared to transverse microtubules and, in consequence, are better substrates for de-tyrosination. This means that the stability of an individual microtubule would depend on its direction.

Outlook: what is the base for direction-dependent stability?

The extent of tubulin de-tyrosination depends on the direction of a given microtubule, providing evidence for direction-dependent stability. The stability of individual microtubules is generally believed to depend on its association with structural MAPs (Bin-Bing and Kirschner, 1999; Caudron *et al*., 2000). In this context, direction-dependent stability would mean that the association of a microtubule with these MAPs depends on direction. This could be achieved by tethering the stabilizing MAPs along a directional field or lattice. Direction and spacing of this lattice would set a default state for maximal microtubule stability. There are three candidates for this type of lattice: (i) the actin cytoskeleton that is oriented with respect to cell axis (Waller *et al*., 2001), similar to the actin phragmosome that acts as spatial 'memory' for the position of the pre-prophase band and guides the re-organization of the microtubular cytoskeleton after completed mitosis (Lloyd, 1991); (ii) the cell wall that is known to stabilize the cortical microtubules (e.g. Fisher and Cyr, 1998); (iii) a subfraction of so-called 'pseudostable' microtubules that are stable in position, but highly dynamic in dimer turnover such that they are easily lost in fixed cells (Himmelspach *et al*., 1999). To understand 'direction' in the context of microtubule re-orientation, it is essential to analyse these candidates for a potential function as directional lattice for microtubule-nucleating or stabilizing factors.

Experimental procedures

Plant material and dose–response assays

Coleoptile segments were obtained as described in Nick *et al*. (1992) from maize coleoptiles (*Zea mays* L. cv Percival) that had been grown for 3 days at 25°C under red light (0.5 W m^{-2}) followed by 1 day in the dark. The excision of segments and the subsequent incubation in the natural auxin, indolyl-3-acetic acid (IAA), took place in the same red light at 25 or 30°C. Growth and microtubule responses were followed for 3 h after the addition of auxin. Depletion from endogenous auxin was achieved by incubation of segments in water for 3 h. Ethyl-*N*-phenylcarbamate (Wako Pure Chemicals, Tokyo, Japan; diluted from a 100-mM ethanolic stock solution), isopropyl-*N*-phenylcarbamate (Sigma-Aldrich, Neu-Ulm, Germany; diluted from a 10-mM ethanolic stock solution), oryzalin (Dow Elanco, Munich, Germany; diluted from a 10-mM stock solution in DMSO), trifluralin (Ag Specialities, Portland, Oregon, USA; diluted from a 10-mM stock solution in DMSO) and colchicin (Sigma, Neu-Ulm, Germany; diluted from a 50-mM aequous stock solution) were added to the medium from stock solutions that were stored at −20°C. Controls containing the respective solvent in a concentration corresponding to that of the highest drug concentration were included throughout the study.

EPC sepharose chromatography and treatment with carboxypeptidase A

Carboxy-ethyl-*N*-phenylcarbamate was synthetized as described in Mizuno *et al*. (1981), and coupled to sepharose 4B (Amersham-Pharmacia, Freiburg, Germany) that had been extended by an aminoethyl linker (Cuatrecasas, 1970). Coleoptile segments were ground by mortar and pestle in liquid nitrogen and a soluble extract produced and fractionated as described in Freudenreich and Nick (1998) using a microtubule-stabilizing buffer (MSB: 25 mM Mes, 5 mM EGTA, 5 mM $MgCl_2$, 1 M glycerol, 1 mM GTP, 1 mM DTT, 1 mM phenylmethylsolphonyl fluoride, 1 μg ml^{-1} leupeptin, pepstatin and aprotinin, pH 6.9). For small samples, the sepharose was filled onto glass wool into 50-μl Eppendorf tips and fractions were collected by centrifugation (1 min, 15 000 ***g***) into small tubes. The fractions were precipitated by trichloroacetic acid (Bensadoun and Weinstein, 1976) prior to processing for SDS-PAGE. For the assembly of microtubules from tyrosinylated tubulin, the fractions were concentrated by ultrafiltration (Centrex UF-2, Schleicher and Schüll, Dassel, Germany) to 1 mg ml^{-1} of total protein. Microtubule assembly was induced in these samples as described in Nick *et al*. (1995). The microtubules were treated with 0.1 units ml^{-1} carboxypeptidase A (C9268, Sigma-Aldrich, Neu-Ulm, Germany) in MSB at 30°C for variable time intervals (0–60 min), the reaction was stopped by transfer to ice and the carboxypeptidase A was washed out by collecting the microtubules by ultracentrifugation (300 000 ***g***, 10 min, 4°C), replacing the supernatant by the same volume of fresh MSB and repeating this step. Then, the microtubule sediment was solubilized on ice by 1 mM $CaCl_2$ in MSB by using a glass rod for 15 min, the sediment was removed by ultracentrifugation (300 000 ***g***, 10 min, 4°C) and the supernatant was assayed by EPC sepharose chromatography. The C-terminal peptide of maize TUBA2 was synthetized (Pepscan Systems, Lelystad, the Netherlands) either in the tyrosinylated form (FDEGEEGDDGDEY) or in the de-tyrosinylated form (FDEGEEGDDGDE) and conjugated to ovalbumin as a carrier via N-terminal cysteine. The peptide was used at 0.5 μg $μl^{-1}$ (in MSB) for EPC sepharose chromatography. In some experiments, the

tyrosinylated conjugate was pre-treated with 0.1 units ml^{-1} carboxypeptidase A (60 min, 30°C) and purified on a sephadex G-25 column prior to EPC sepharose chromatography.

Double visualization of the DM1A and the ATT epitope

Maize epidermal strips were processed for double immunofluorescence as described in Nick *et al.* (1995) and visualized by confocal laser scanning microscopy (DM RBE; Leica, Bensheim, Germany) using a dual-wavelength configuration with excitation by the 488-nm and the 568-nm line of an argon–krypton laser, a beam splitter at 575 nm and barrier filters at 580 and 590 nm and a line algorithm averaging 32 individual scans. The ATT or YL1/2 antibodies were added first, followed by an incubation with TexasRed-conjugated antimouse IgG (or antirat IgG in case of the YL1/2). In a third step, the DM1A epitope was labelled using a FITC conjugate of DM1A. The specimens were blocked and washed extensively prior to each incubation as described in Nick *et al.* (1995). As negative control, the sections were treated with 0.1 units ml^{-1} carboxypeptidase A (60 min, 30°C) prior to incubation with the primary antibody. Additional controls included samples where the primary antibody was replaced by the respective serum from unchallenged animals (Figure 5a, right-hand panel).

Antibodies

The mouse monoclonal antibody DM1A (Sigma, Neu-Ulm, Germany) was used to detect de-tyrosinylated α-tubulin in a dilution of 1 : 300 for Western blotting and a FITC conjugate of DM1A in a dilution of 1 : 50 for immunofluorescence. The mouse monoclonal antibody ATT (Kreis, 1987; purchased from Sigma, Neu-Ulm, Germany) and the rat monoclonal antibody YL1/2 (Kilmartin *et al.*, 1982; purchased from Biozol, Eching, Germany) were used to detect tyrosinylated α-tubulin in a dilution of 1 : 500 for Western blotting and 1 : 50 for immunofluorescence. Peroxidase-conjugated antibodies against mouse IgG were used in a dilution of 1 : 2500 to visualize tubulin in Western blots; TexasRed-conjugated antimouse IgG (for YL1/2) or antimouse IgG (for ATT) were purchased from Molecular Probes (Eugene, OR, USA) and used in a dilution of 1 : 25 for immunofluorescence.

Acknowledgements

This work was supported by the Nachwuchsgruppen Programme of the Volkswagen Foundation (Dynamics of the Plant Cytoskeleton) to PN and funds from the Deutsche Forschungsgemeinschaft (Programme 'Molecular Analysis of Phytohormone Action') to QYW.

References

Bensadoun, A. and Weinstein, D. (1976) Assay of proteins in the presence of interfering materials. *Anal. Biochem.* **70**, 241–250.

Bin-Bing, Z.H. and Kirschner, M.W. (1999) Quantitative measurement of the catastrophe rate of dynamic microtubules. *Cell Motility Cytoskeleton*, **43**, 43–51.

Breitling, F. and Little, M. (1986) Carboxy-terminal regions on the surface of tubulin and microtubules. Epitope locations of YOL1/34, DM1A and DM1B. *J. Mol. Biol.* **189**, 367–370.

Caudron, N., Valiron, O., Usson, Y., Valiron, P. and Job, D. (2000) A reassessment of the factors affecting microtubule assembly and disassembly *in vitro*. *J. Mol. Biol.* **297**, 211–220.

Cuatrecasas, P. (1970) Protein purification by affinity chromatography: derivatization of agarose and polyacrylamide beads. *J. Biol. Chem.* **245**, 3059–3065.

Duckett, C.M. and Lloyd, C.W. (1994) Gibberellic acid-induced microtubule orientation in dwarf peas is accompanied by rapid modification of an α-tubulin isotype. *Plant J.* **5**, 363–372.

Fisher, D.D. and Cyr, R.J. (1998) Extending the Microtubule/Microfibril Paradigm: cellulose is required for normal microtubule alignment in elongating cells. *Plant Physiol.* **116**, 1043–1051.

Freudenreich, A. and Nick, P. (1998) Microtubular organization in tobacco cells: heat shock protein 90 can bind to tubulin *in vitro*. *Bot. Acta*, **111**, 273–279.

Himmelspach, R., Wymer, C.L., Lloyd, C.W. and Nick, P. (1999) Gravity-induced re-orientation of cortical microtubules observed *in vivo*. *Plant J.* **18**, 449–453.

Joyce, C.M., Villemur, R., Snustad, D.P. and Silflow, C.D. (1992) Tubulin gene expression in maize *Zea mays* L. Change in isotype expression along the developmental axis of seedling root. *J. Mol. Biol.* **227**, 97–107.

Khawaja, S., Gundersen, G.G. and Bulinski, J.C. (1988) Enhanced stability of microtubules enriched in de-tyrosinylated tubulin is not a direct function of de-tyrosination level. *J. Cell Biol.* **106**, 141–149.

Kilmartin, J.V., Wright, B. and Milstein, C. (1982) Rat monoclonal antitubulin antibodies derived by using a new non-secreting rat cell line. *J. Cell Biol.* **93**, 576–582.

Kreis, T.E. (1987) Microtubules containing de-tyrosinylated tubulin are less dynamic. *EMBO J.* **6**, 2597–2606.

Kumar, N. and Flavin, M. (1981) Preferential action of a brain detyrosinolating carboxypeptidase on polymerized tubulin. *J. Biol. Chem.* **256**, 7678–7686.

Lloyd, C.W. (1991) Cytoskeletal elements of the phragmosome establish the division plane in vacuolated plant cells. In *The Cytoskeletal Basis of Plant Growth and Form* (Lloyd, C.W., ed.). London: Academic Press, pp. 245–257.

Lloyd, C.W. (1994) Why should stationary plant cells have such dynamic microtubules? *Mol. Biol. Cell*, **5**, 1277–1280.

Lloyd, C.W. and Seagull, R.W. (1985) A new spring for plant cell biology: microtubules as dynamic helices. *Trends Biochem. Sci.* **10**, 476–478.

MacRae, T.H. (1997) Tubulin post-translational modifications – enzymes and their mechanisms of action. *Eur. J. Biochem.* **244**, 265–278.

Mizuno, K., Koyama, M. and Shibaoka, H. (1981) Isolation of plant tubulin from adzuki bean epicotyls by ethyl *N*-phenylcarbamate-Sepharose affinity chromatography. *J. Biochem.* **89**, 329–332.

Mizuno, K. and Suzaki, T. (1991) Effects of anti-microtubule drugs on *in vitro* polymerization of tubulin from mung bean. *Bot. Mag. Tokyo*, **103**, 435–448.

Nick, P. (1998) Signaling to the microtubular cytoskeleton in plants. *Int. Rev. Cytol.* **184**, 33–80.

Nick, P., Bergfeld, R., Schäfer, E. and Schopfer, P. (1990) Unilateral reorientation of microtubules at the outer epidermal wall during photo and gravitropic curvature of maize coleoptiles and sunflower hypocotyls. *Planta*, **181**, 162–168.

Nick, P., Lambert, A.M. and Vantard, M. (1995) A microtubule-associated protein in maize is induced during phytochrome-dependent cell elongation. *Plant J.* **8**, 835–844.

Nick, P., Schäfer, E. and Furuya, M. (1992) Auxin redistribution during first positive phototropism in corn coleoptiles – microtubule re-orientation and the Cholodny-Went Theory. *Plant Physiol.* **99**, 1302–1308.

Skoufias, D.A. and Wilson, L. (1998) Assembly and colchicine binding characteristics of tubulin with maximally tyrosinylated

and de-tyrosinylated alpha-tubulins. *Arch. Biochem. Biophysics*, **351**, 115–122.

Waller, F., Wang, Q.Y. and Nick, P. (2001) Actin and signal-controlled cell elongation in coleoptiles. In *Actin: a Dynamic Framework for Multiple Plant Cell Functions.* (Staiger, C.J., Baluška, F., Volkmann, D., Barlow, P., eds). Dordrecht: Kluwer, pp. 477–496.

Watts, D.I., Monteiro, M.J. and Cox, R.A. (1987) Identification of Eco-RV fragments spanning the *n*-alpha tubulin gene of *Physarum*. *FEBS Lett.* **241**, 229–233.

Wehland, J. and Willingham, M.C. (1983) A rat monoclonal antibody reacting specifically with the tyrosylated form of alpha-tubulin. Part II. Effects on cell movement, organization of microtubules, and intermediate filaments, and arrangement of Golgi elements. *J. Cell Biol.* **97**, 1476–1490.

Yuan, M., Shaw, P.J., Warn, R.M. and Lloyd, C.W. (1994) Dynamic re-orientation of cortical microtubules from transverse to longitudinal, in living plant cells. *Proc. Natl Acad. Sci. USA*, **91**, 6050–6053.